Optimum color filters for CCD digital cameras

Kai Engelhardt and Peter Seitz

A procedure for the definition of optimum spectral transmission curves for any solid-state (especially silicon-based CCD) color camera is presented. The design of the target curves is based on computer simulation of the camera system and on the use of test colors with known spectral reflectances. Color errors are measured in a uniform color space (**CIELUV**) and by application of the Commission Internationale de l'Eclairage color difference formula. Dielectric filter stacks were designed by simulated thermal annealing, and a stripe filter pattern was fabricated with transmission properties close to the specifications. Optimization of the color transformation minimizes the residual average color error and an average color error of ~ 1 just noticeable difference should be feasible. This means that color differences on a side-to-side comparison of original and reproduced color are practically imperceptible. In addition, electrical cross talk within the solid-state imager can be compensated by adapting the color matrixing coefficients. The theoretical findings of this work were employed for the design and fabrication of a high-resolution digital CCD color camera with high colorimetric accuracy.

Key words: Colorimetry, dielectric filter, CCD, digital color camera.

1. Introduction

The human visual system is a complex and largely still ill-understood image data acquisition and processing system. It is a fortunate fact that the rich human visual color perception is accurately described by a simple trireceptor theory that involves the linear combination of only three different photoreceptor types with known spectral sensitivity. For this reason today's color measurement and color reproduction technology has reached quite a high performance. Most modern techniques for acquisition and rendering of color imagery, however, still produce color pictures perceptibly different from the original scene. A major reason for this is the difficult selection and fabrication of transmission filter sets that are suitable for incorporation into color television cameras and color scanners. The present work describes an attempt at designing and producing dielectric filter sets that are either optimum in an absolute, theoretical sense, or close to this optimum and robust to fabrication tolerances at the same time.

What is normally done for consumer color video cameras and color scanners[1] is that, for a given sensor spectral response, the illumination's spectrum and the chromaticities of the reproduction primaries [e.g., the phase alternation line (PAL) or national television systems committee (NTSC) monitor's phosphors] theoretically optimum filter triplet characteristics are determined, and—because of fabrication limitations and cost—one tries to match them with dye mosaic filters as well as possible. In broadcast cameras with their increased performance requirements three-chip solutions are adopted by using prisms with standard design dielectric filters.

According to the trireceptor theory of human color vision one needs only the signals from three different receptors with an all-positive response, the so-called tristimulus or color-matching curves, to predict the color perception of the human visual system and to reproduce this color stimulus accurately by using suitable color primaries. Because of the linearity of the system, any linear combination of the color-matching curves is also sufficient, and it is always possible to form linear combinations of these signals (so-called matrixing) that can be used directly for the (additive) reproduction of a color stimulus. In this way perfect color reproduction is possible, in principle, within the reproduction capabilities of the output device. Since there are infinitely many possibilities of obtaining linear combinations of the color-matching curves with an all-positive transmission, the question to be answered in this work is which of these linear combinations (for which ideal matrixing coefficients can be determined for all perceptible colors) should be selected. Two selection criteria are investigated in this work; first, the theoretical optimum

The authors are with the Paul Scherrer Institute Zürich, Badenerstrasse 569, CH-8048 Zurich, Switzerland.

Received 27 May 1992.
0003-6935/93/163015-09$06.00/0.

with respect to minimum perceptible color noise caused by the unavoidable photon noise, and second, small perceptible color noise (close to the theoretical optimum) but for which it is possible to fabricate good dielectric transmission filters with their normal fabrication tolerances.

The presented theoretical studies were applied to the development of the prototype[2] of an advanced desktop publishing color camera system as part of the European research initiative ESPRIT (European Strategic Program for Information Technology) II project 2103 MASCOT (Multienvironment Advanced System for Colour Treatment). Dielectric filters were designed and fabricated according to target transmission curves that were obtained from our simulations, taking into account the illumination's spectrum and the sensor's spectral sensitivity. Residual colorimetric errors were minimized by matrixing, reducing the effects of the nonideal filter fabrication and inaccuracies in the measurement of the sensor's spectral sensitivity.

2. Baseline for Filter Design

The goal of this work was to provide the theoretical framework for the design of color filters for a high-resolution digital still camera with high colorimetric accuracy. Such a camera would find many practical applications in desktop publishing, the graphic arts, the printing industry, and the medical area. These applications determine the boundary conditions for which the performance of the camera should be optimized.

Since color can be represented unambiguously by a vector with only three components, three individual detectors (pixel types), K, L, M, with suitably chosen spectral responses are sufficient to determine the locus of each color within the space of perceivable colors. If a camera should be capable of perfect colorimetric reproduction of objects, three-color channels must be established with spectral responses equal to a set of linear combinations of the standard color-matching functions $\bar{x}$, $\bar{y}$, $\bar{z}$. Usually images of highly structured objects are acquired with the camera. Because the individual colored fields are viewed under only a small angle, the 2° color-matching functions[3] [CIE (Commission Internationale de l'Eclairage) 1931] apply.

The main fields of application for this color camera share the availability of high levels of illuminance with a suitable spectral distribution. Therefore, in contrast to consumer video cameras, the filter set should be optimized for bright-light conditions to achieve minimum color errors from photon noise.

To achieve programmable, high spatial resolution, the camera incorporates a scanning mechanism with which the scene can be shifted laterally with respect to the $1k \times 1k$ pixel CCD chip (Thomson THX 31156) employed. This is realized with an optical microscan module that forms part of the lens system, which consists of a parallel glass plate that can be tilted in small steps around two orthogonal axes. In this way, not only can the spatial resolution of the camera be significantly enhanced but it also becomes possible to expose a scene in three steps so that every detail of the scene can be seen through three different color filters, arranged in a certain pattern on top of the pixels. The arrangement of color filters chosen for this purpose is simple vertical stripes, making crosstalk corrections easier and avoiding complex color decoding algorithms and antialiasing measures such as the ones required for the shift patterns."[4] The reason for selecting patterned color filters instead of sequential exposure through uniform, large-area filters was the desire to use the camera also for single-shot color exposures of moving objects, albeit at reduced spatial resolution. For a detailed description of the complete camera system see Ref. 2.

3. Design of the Filter Transmission Curves

The color filters were realized as multilayer dielectric filters arranged as stripes on a glass substrate and glued onto the top of the CCD imager. The application of advanced filter design techniques by using simulated thermal annealing[5,6] allows almost any desired filter transmission characteristic to be achieved. Only fabrication tolerances represent a limitation for the practicability of a certain filter set.

A. Simulation Model of the System

The camera was simulated by using the simplified model shown in Fig. 1. The object is illuminated with a known spectral power distribution $S(\lambda)$. Light reflected by the object is modified by the spectral reflectance $\rho(\lambda)$, and a certain amount passes the lens and the infrared cutoff filter with spectral transmittances $\tau_{\text{lens}}(\lambda)$ and $\tau_{\text{IR}}(\lambda)$. The spectral transmittances and the spectral response $s_{\text{CCD}}(\lambda)$ of the CCD array are multiplied and normalized to obtain the basic spectral response $s_{\text{b/w}}(\lambda)$ of the camera without color filters:

$$s_{\text{b/w}}(\lambda) \propto \tau_{\text{lens}}(\lambda) \times \tau_{\text{IR}}(\lambda) \times s_{\text{CCD}}(\lambda). \quad (1)$$

Figure 2 displays these spectral distributions that are basic to our filter design. At short wavelengths the spectral response $s_{\text{b/w}}(\lambda)$ is determined mainly by the

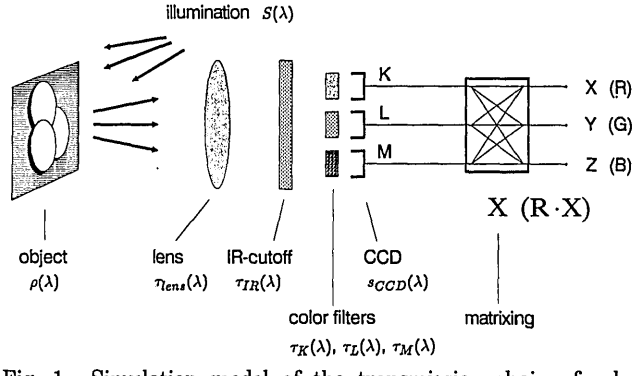

Fig. 1. Simulation model of the transmission chain of color information.

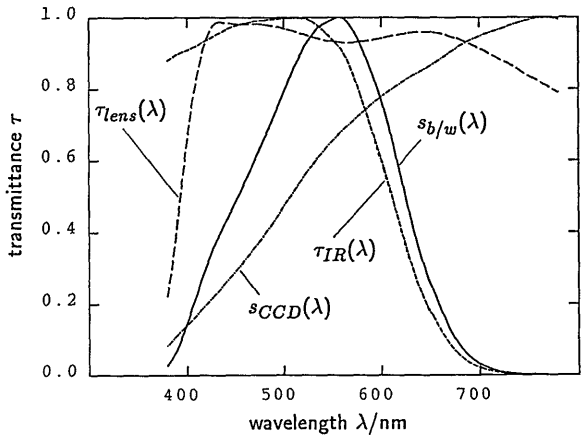

Fig. 2. Normalized basic spectral response $s_{b/w}(\lambda)$ of the camera composed of the spectral response $s_{CCD}(\lambda)$ of the CCD image sensor, and the spectral transmissions $\tau_{ens}(\lambda)$ of the lens and $\tau_{IR}(\lambda)$ of the infrared cutoff filter.

spectral response of the CCD array and at long wavelengths by the infrared cutoff filter.

For each color channel K, L, M the spectral response $s_{b/w}(\lambda)$ is further multiplied by the transmittances $\tau_K(\lambda)$, $\tau_L(\lambda)$, $\tau_M(\lambda)$ of the color filters to yield the spectral responses $s_K(\lambda)$, $s_L(\lambda)$, $s_M(\lambda)$. In the MASCOT digital CCD camera the video signal is digitized pixel synchronously by a 10-bit analog–digital converter at a measured nonlinearity of 67 dB.[7] Color transformation and any subsequent signal processing are performed in the digital domain. The effects of quantization on the colorimetric performance of the camera are discussed in Section 6.

B. Estimation of Colorimetric Performance and Matrixing

Given the transmission spectra $\tau_K(\lambda)$, $\tau_L(\lambda)$, $\tau_M(\lambda)$ of a special filter triplet the colorimetric performance of the camera can be checked by computer simulation if a set of test colors is provided with known spectral reflectances. Each test color will modify the spectrum of illuminance according to its spectral reflectance $\rho(\lambda)$. For the spectrum of illuminance $S(\lambda)$ we used the spectrum of average daylight D_{65}, a CIE standard.[3] In a first step the resulting spectrum is multiplied by the corresponding values $\bar{x}(\lambda)$, $\bar{y}(\lambda)$, $\bar{z}(\lambda)$ of the standard color-matching functions and summed over wavelength λ to obtain the (X_R, Y_R, Z_R) tristimulus values of the test color as a reference. The summation was carried out at intervals $\Delta\lambda$ of 5 nm from 380- to 780-nm wavelength.

In a second step the values from the standard color-matching functions are substituted by values from the spectral responses of the camera $s_K(\lambda)$, $s_L(\lambda)$, $s_M(\lambda)$ to obtain tristimulus values (K, L, M) measured at the output of the CCD array. A linear transformation matrix $\mathscr{X}$ is applied to color vector (K, L, M) to obtain tristimulus values (X_C, Y_C, Z_C) in the CIE 1931 *XYZ* system at the output of the simulated camera.

If the responses of the color channels K, L, M show deviations from a set of linear combinations of $\bar{x}, \bar{y}, \bar{z}$ or if noise affects the tristimulus values (K, L, M), then no linear transformation **X** can be found to produce correct tristimulus values (X_C, Y_C, Z_C) for all test colors simultanously.

To estimate the resulting color error for each test color we transformed the color vectors from both steps (nonlinearly) from the CIE 1931 *XYZ* space to a uniform color space in which color differences are perceived approximately uniformly:

$$(X_R, Y_R, Z_R) \mapsto (L_R^*, u_R^*, v_R^*),$$
$$(X_C, Y_C, Z_C) \mapsto (L_C^*, u_C^*, v_C^*).$$

In our simulation the CIE 1976 L^*, u^*, v^* system[3] (CIELUV) was employed but, in general, results that were obtained by using the CIE 1976 L^*, a^*, b^* system[3] (CIELAB) proved to be similar.

Next, the distance of both color vectors in the uniform color space was calculated by using the CIE color difference formula[3] to obtain the colorimetric error ΔE for the reproduction of each test color:

$$\Delta E = [(L_R^* - L_C^*)^2 + (u_R^* - u_C^*)^2 + (v_R^* - v_C^*)^2]^{1/2}. \quad (2)$$

If the spectral responses of the three-color channels deviate from any set of linear combinations of the standard color-matching functions, optimization[8] of the color transformation matrix will help to minimize the systematic color error of the camera. For minimum perceivable color errors a nonlinear optimization in the uniform color space (CIELUV or CIELAB) must be carried out. The following procedure, which is similar to that presented in Ref. 1, proved to be efficient: In a first step a color transformation matrix $\mathscr{X}$ is determined that minimizes the mean quadratic error of the reproduced test colors in *XYZ* space. In this linear optimization three systems of linear equations have to be solved. In a second step a nonlinear optimization based on the method of steepest descent is applied that uses a variable step width to decrease the total number of steps. As an initial transformation matrix for the nonlinear optimization we use the matrix that resulted from linear optimization. We obtain a matrix $\mathscr{X}_{opt}$ for the transformation of detector tristimulus vector (K, L, M) to tristimulus vector (X, Y, Z) in the standard *XYZ* space that minimizes the perceivable color errors at the output device. If, for example, colors should be displayed on a red–green–blue (RGB) monitor with PAL phosphor primaries, then the final transformation matrix results from the matrix product $\mathscr{R}_{PAL}\mathscr{X}_{opt}$, where matrix $\mathscr{R}_{PAL}$ performs the transformation to the specific output device including an optional shift in reference white.

The mean color error that results for a special set of filters strongly depends on the set of test colors that is used to optimize the camera's performance. Our set of test colors consists of approximately 300 carefully selected colors at various relative luminous reflectances with most of them highly saturated. The loci in the CIE chromaticity diagram of the various test

colors are shown in Fig. 3. The set includes the CIE standard test colors (indicated by • in Fig. 3) that are required to calculate the CIE general color rendering index[3] R_a, optimal colors[3] (indicated by + in Fig. 3) of different dominant wavelength, and luminous reflectance as well as a subset of 200 samples of test colors (indicated by △, ○, ▽ in Fig. 3) from the commercially available *COLORCURVE*[9] *ATLAS*. Optimal colors were included in the simulation because these colors represent the theoretic limit of object colors under the given spectrum of illumination and, for medium and low relative luminous reflectances, are localized far outside the color triangle defined by the chromaticity coordinates of the three primaries of the monitor. Such colors cannot be reproduced correctly on a monitor, but the camera can be used to measure their color coordinates. Colors from the Colorcurve system are especially suited for the design of color filters by computer simulation because spectra of reflectance are provided for each color sample and, after realization, actual performance can be investigated by using the real color samples. The spectra of reflectance of the Colorcurve colors are provided from 400 to 700 nm in steps of 20 nm accompanied by tristimulus values in the CIE 1964 *XYZ* system of the 10° standard observer under illuminant D_{65}. Our simulation works with spectral data from 380 to 780 nm in steps of 5 nm. Therefore, the original data must be extrapolated and then interpolated. In Ref. 10 various techniques for extrapolations of truncated spectra are presented. In contrast to these automatic techniques that follow fixed rules, we prefer to add reasonable looking values at both limiting wavelengths by hand for extrapolation and to interpolate the spectra at 5-nm intervals by using a cubic spline interpolation. Finally we checked if the manipulated spectra still represent the original colors that exist as real samples and, if necessary, the procedure was repeated by using improved values in the extrapolation. For a check of the manipulated spectra, we calculated their tristimulus values in the CIE 1964 *XYZ* system under illuminant D_{65} and compared these results with the original data provided by Colorcurve Systems.

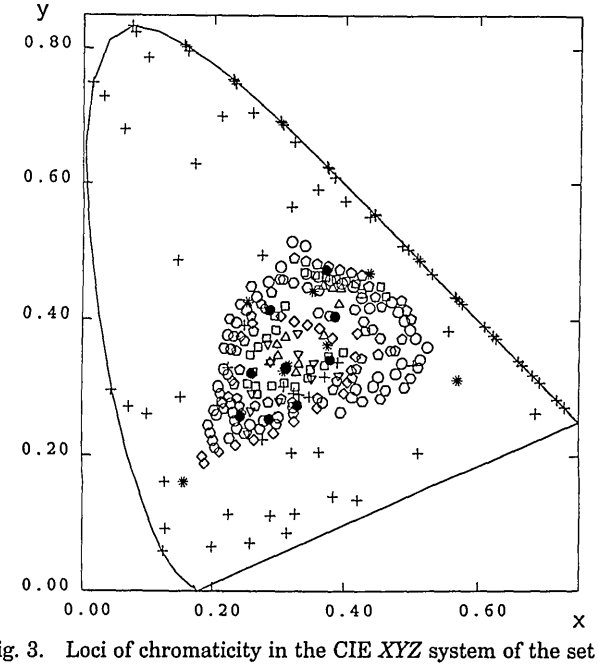

Fig. 3. Loci of chromaticity in the CIE *XYZ* system of the set of test colors used in simulation and optimization. The set consists of the CIE standard test colors (•), optimal colors (+) of different luminous reflectances, and a subset of 200 samples of test colors from the COLORCURVE ATLAS at different levels of luminous reflectance (△, ○, ▽′).

The optimization of matrixing was carried out over the subset of Colorcurve test colors only. All values ΔE of estimated average colorimetric performance that are given in the following sections were obtained after nonlinear optimization of matrixing.

C. Filter Triplet for Optimum Noise Performance

For the target fields of application of the camera the filter triplet should be optimized for high levels of illuminance. Therefore one goal is to find three filter transmission curves and the corresponding color transformation matrix that are matched to a specific output device and show minimum color error at the output that originates from temporal noise in the photodetector. At high levels of illuminance Poisson-distributed photon noise predominates. As outlined before, the filter transmission curves must be chosen such that the basic spectral response $s_{b/w}(\lambda)$ of the camera is modified to yield spectral responses of the color channels that are linear combinations of the color-matching functions.

Any linear combination of the color-matching functions can be addressed in the following way: Each color channel is replaced by an imaginary primary stimulus that emits light of a spectral power distribution that is equal to the spectral response. The chromaticity coordinates (x, y, z) of the three imaginary primary stimuli must be selected to be linearly independent of each other. By solving a system of linear equations the basic linear transformation $\mathscr{A}$ can be derived from these chromaticity coordinates. The spectral response curves of the color channels are obtained if the inverse transformation matrix $\mathscr{A}^{-1}$ is applied to the color-matching functions $\bar{x}$, $\bar{y}$, $\bar{z}$. Nonnegative response curves that can be realized by using a photodetector and filters are obtained automatically only if the triangle in the x-y plane formed by the chromaticity loci of the three imaginary primary stimuli contains the spectrum locus completely.

The colorimetric quality of the individual filter triplets that are determined by this procedure differs only in the noise performance. To check noise performance in the simulation we disturbed the tristimulus values (K, L, M) of each test color by a set of 125 disturbance vectors that approximate a Gaussian amplitude distribution in each color channel to simulate the temporal noise from each detector element. The temporal noise consists mainly of photon noise, noise from a dark signal, and read noise that originates from the on-chip output amplifier of the CCD

imager. The number $n_{i,k}$, $k = K, L, M$ of photogenerated electrons of each pixel is proportional to the component of the tristimulus value (K_i, L_i, M_i) of test color i that corresponds to the specific color of the pixel; e.g., $n_{i,K} = n_{e^-} \times K_i$.

The conversion factor n_{e^-} is given by the convention that a tristimulus component of 100 is equivalent to a saturated detector element with a number of photoelectrons given by the full well capacity of the CCD imager. In addition the detector element is filled with the number n_{ds} of electrons that are generated by dark current that is sensitive to temperature and proportional to the sum of the integration time of the imager and the time required for read out. The temporal noise voltage of each pixel is proportional to the square root of the total number of electrons collected in the pixel. Because this noise voltage is independent of the noise voltage that is generated by the output amplifier, these voltages must be added like vectors and the standard deviation $\sigma_{i,k}$ of signal electrons from each pixel can be calculated for each test color i; e.g., for color channel K

$$\sigma_{i,K} = \{[(n_{i,K} + n_{ds})^{1/2}]^2 + n_{\text{read}}^2\}^{1/2}. \tag{3}$$

The number n_{read} of noise electrons contributed by the output amplifier is obtained if the noise voltage of read noise is converted to electrons by using the conversion factor F of the output amplifier, which gives the output voltage change per signal electron and which typically is of the order of 1 $\mu V/e^-$.

The Gaussian amplitude distribution was approximated by the five discrete amplitudes $-1.4\sigma_{i,k}$, $-0.53\sigma_{i,k}$, 0, $+0.53\sigma_{i,k}$, $+1.4\sigma_{i,k}$, which follow if the area under the Gaussian function is divided into five regions of equal area and the center of gravity is determined for each of these regions. The combination of these five discrete noise amplitudes for each component k gives a set of 125 different noise vectors, which backconverted to the KLM space, represent an isotropic disturbance of the tristimulus vector (K_i, L_i, M_i) of test color i as shown schematically in Fig. 4(a). To estimate the effect of temporal noise on color reproduction of the CCD still camera we must transform the whole set of disturbed tristimulus vectors to the uniform color space for each test color. By using this transformation the isotropic disturbance of the color vector in general is changed to an anisotropic disturbance that may look like the one shown in Fig. 4(b). For each test color i the colorimetric effect of temporal noise can be described by a difference vector $\mathbf{\Delta E_i}$ in the uniform color space that indicates the magnitude and direction of the perceived color shift by noise and that is calculated by averaging over the color shift vectors $\mathbf{\Delta E_{i,j}}$, $\mathbf{j} = 1 \ldots 125$:

$$\mathbf{\Delta E_i} = \frac{1}{125}\sum_{j=1}^{125} \mathbf{\Delta E_{i,j}},$$

$$\mathbf{\Delta E_{i,j}} = (\mathbf{\Delta L_{i,j}}^*, \mathbf{\Delta u_{i,j}}^*, \mathbf{\Delta v_{i,j}}^*). \tag{4a}$$

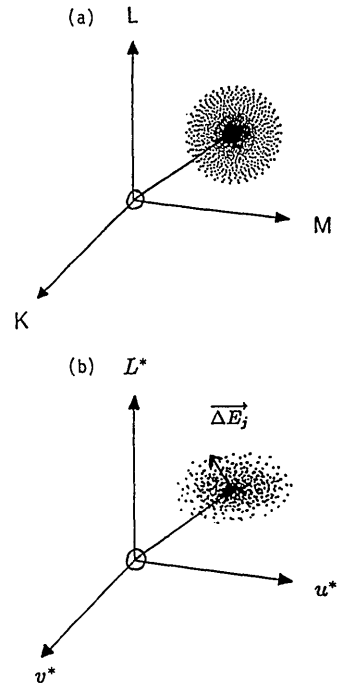

Fig. 4. (a) Illustration of an isotropic disturbance of the tristimulus vector (K_i, L_i, M_i) in the detectors KLM space by photon noise, noise from a dark signal, and read noise. (b) Illustration of the anisotropic disturbance of the color vector resulting from the nonlinear transformation of the isotropic disturbances in KLM space (a) to a uniform color space, for example, the CIELUV space.

From all the individual color shift vectors $\mathbf{\Delta E_{i,j}}$ we can calculate the value of the average color error ΔE_i from temporal noise for test color i and finally the total color error ΔE_{noise} that is due to noise that is averaged over the set of N test colors:

$$\Delta E_i = \frac{1}{125}\sum_{j=1}^{125} (\mathbf{\Delta E_{i,j}} \cdot \mathbf{\Delta E_{i,j}})^{1/2}, \tag{4b}$$

$$\Delta E_{\text{noise}} = \frac{1}{N}\sum_{i=1}^{N} \Delta E_i. \tag{4c}$$

This evaluation procedure is applied to many different filter sets and we find a filter triplet that, for the specific CCD imager in our application, provides the minimum color errors from temporal noise. In Fig.5(a) the dotted curves show the target spectral transmission characteristics of the filter triplet; the solid curves show the transmission characteristics of the filter triplet that results from the design of the dielectric filter stacks by simulated thermal annealing.[5,6]

Assuming an integration time of 250 ms, a read time of 240 ms, and a maximum saturation of 80% full well, a total color error ΔE_{noise} of 1.1 jnd (CIELUV) for the subset of Colorcurve test colors results, which is just above the human discrimination threshold for colors and which would be difficult to detect. A general color rendering index R_a of 95 is found if only noise is taken into account. The average color shift

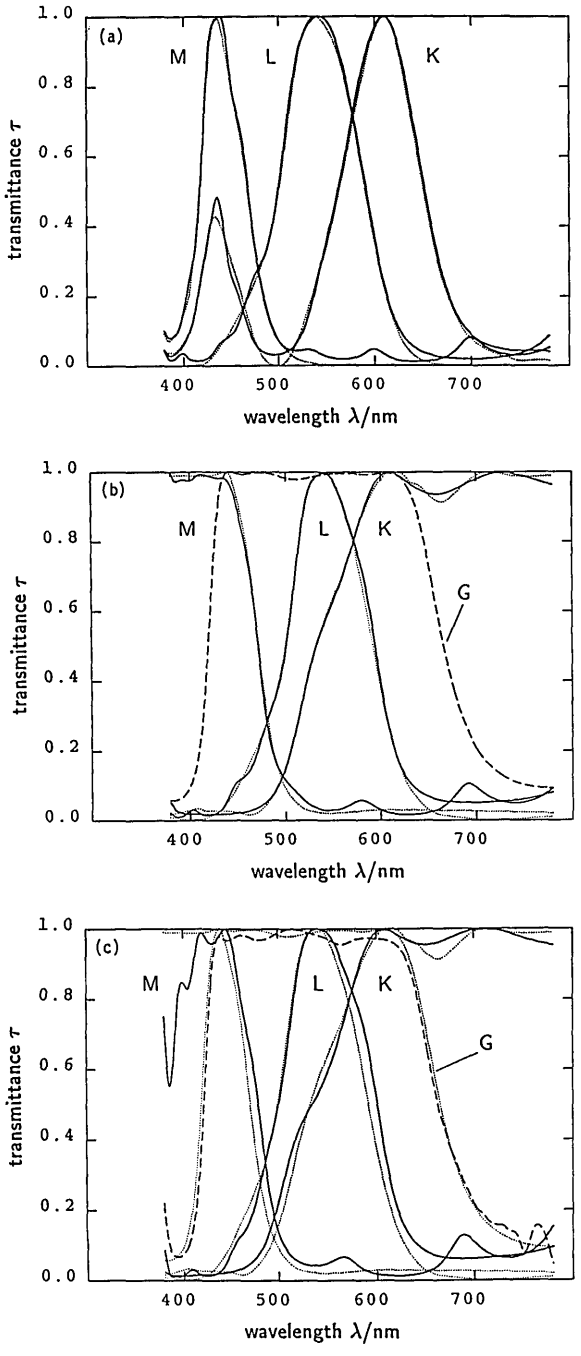

Fig. 5. (a) Filter triplet for optimum noise performance: target spectral transmission (dotted curve) and spectral transmission curves of the designed dielectric filter stacks (solid curve). (b) Optimum practical filter set: target spectral transmission (dotted curve) and spectral transmission curves of the designed dielectric filter stacks (solid curve). The additional global filter G (dashed curve) is deposited onto a separate substrate and inserted into the imaging path to prefilter the light of all the color channels. (c) Optimum practical filter set: target spectral transmission (dotted curve) and spectral transmission of the fabricated dielectric filters K, L, M (solid curve) and the global filter G (dashed curve).

$|\Delta \mathbf{E}_i|$ was calculated to be extremely low and for no color i exceeds 0.02 jnd. Under the same conditions the signal-to-noise ratio was calculated for PAL RGB output signals and the spectrum of illuminant D_{65}. The signal to noise ratio was 43 dB for the red channel, 50 dB for the green channel, and 45 dB for the blue channel.

The transmission curves obtained from the discussed filter design show only slight departures from the target transmission curves as can be seen in Fig. 5(a). The application of the designed filter triplet's spectra in the simulated camera gives a systematic color error ΔE of 0.8 jnd (CIELUV). The general color rendering index R_a is calculated to be 97.

The design of the dielectric filter stacks shows that this filter triplet would be difficult to manufacture with tight tolerances, especially if the filter stacks of the individual colors have to be deposited sequentially onto the same substrate to produce a patterned stripe filter. For each of the three filter stacks the design demands 21 layers with total stack heights between 1.44 and 1.77 μm. If fabrication tolerances are taken into account this filter triplet surely is not optimum.

D. Optimum Practical Filter Set: Global Filter Concept

In general, dielectric filters are easier to design and fabricate if the spectral region decreases in which the filter must match a desired target transmission especially at short wavelengths. Therefore we decided to add a global filter to the triplet of color filters. This global filter covers all the detector elements and is deposited on a separate substrate, which in our case is the infrared cutoff filter. The global filter defines the transmission edges of the whole filter set in the blue and in the red. Because of this additional filter two of the three color filters become much simpler and the sequential deposition of the patterned stripe filter can be performed with a higher precision.

Furthermore, we searched for a filter triplet with a blue filter M with a transmission of a few percent in the long-wavelength spectral range because design of the dielectric filter stacks becomes less critical if nearly zero transmission in this range is not required. The transmission characteristics of the filter set we found are shown in Fig. 5(b); the dotted curves display the target transmissions, the solid curves show the transmission curves that result from the design of the filter stacks. The dashed curve illustrates the spectral transmission of the designed global filter G that requires 12 dielectric layers with a total thickness of 1.1 μm. The filter of the red channel K is composed of 13 layers with a total thickness of 0.74 μm. The filters of the green and blue channels L and M require 19 layers each with a total thickness of 1.35 and 1.47 μm, respectively.

If the target transmission characteristics are combined with the camera's basic spectral response $S_{b/w}$, the resulting spectral responses s_K, s_L, s_M are no longer a numerically exact linear combination of $\bar{x}$, $\bar{y}$, $\bar{z}$ because the initial target filter transmission data were smoothed by using cubic spline approximation. Target transmission data were obtained that showed no artificial sharp edges or spectral regions of constant transmission both of which would complicate

the design of the dielectric stacks. Target and design curves are in good agreement and from both sets of data a mean colorimetric error ΔE of ~ 1.0 jnd (CIELUV) is calculated after nonlinear optimization of matrixing. The general color rendering index R_a is calculated to be 97.

Noise performance of this filter triplet is estimated to be only slightly worse than that of the previous theoretically ideal filter triplet. Under the same conditions a total color error ΔE_{noise} of 1.3 jnd (CIELUV) is calculated for the subset of Colorcurve test colors. Color errors from noise only produce a general color rendering index R_a of 95. The average color shift $|\Delta \mathbf{E}_i|$ is again lower than 0.02 jnd for every color i. The signal-to-noise ratio for PAL RGB output signals and D_{65} illuminant is calculated to be 41 dB for the red channel, 49 dB for the green channel, and 45 dB for the blue channel.

4. Filter Fabrication and Characterization

The dielectric filters were fabricated by e-beam deposition of TiO_2 and SiO_2; see, for example, Ref. 11. First, the global filter was deposited onto the infrared cutoff filter. The dashed curve in Fig. 5(c) shows its spectral transmission versus the dotted design characteristics. The color filters were deposited onto on a thin glass substrate that was subsequently glued directly onto the CCD imager. For optimum colorimetric reproduction the green filter L was the most critical and was therefore fabricated as the first of the patterned stripe filter to allow a maximum number of trials. Figure 5(c) shows the spectral transmission characteristics of the fabricated filters as solid curves versus the design curves that are dotted. Design and realization are in fairly good agreement.

5. Compensation of Color Cross Talk

Color cross talk occurs from photons that enter the filter of a specific color channel and the photogenerated charge carriers travel inside the silicon of the CCD array such a distance that detection takes place in the pixel of a different color channel. The mean distance that a charge carrier will travel in silicon is higher for longer wavelengths because the long-wavelength photons are absorbed deeper in the silicon. Therefore the amount of cross talk differs for photons that entered different color filters and color errors will arise. The largest cross talk is expected from channel K; the lowest from channel M. Because color cross talk is linearly dependent on intensity it can be compensated almost completely by a linear transformation that may be combined with the color transformation matrix $\mathscr{A}$.

In all modes of the MASCOT camera each image sampling area is digitized subsequently by a pixel of each of the three-color channels to obtain color samples K, L, and M of each sampling area. Since cross talk influences each acquired image in itself, it should be corrected for after each single microscanning step. In contrast, the color transformation will be applied to tristimulus values (K, L, M) that come from different microscanning steps. But if the object color in the image on the CCD array varies smoothly from pixel to pixel and the imaging conditions remain fixed, then, nevertheless, color cross talk can be removed almost completely.

Because color cross talk is a linear effect it can be measured by the projection of a suitable spot of white light subsequently onto a K, an L, and an M pixel. The spot ideally should have the same size and shape as the photosensitive part of a pixel. Since in our case the pixels were additionally masked with a chrome mask that left only the center part of the pixel area photosensitive ($\sim 25\%$ of the pixel area), it was easy to achieve this in practice. With no cross talk present three tristimulus vectors (K, L, M) are obtained that, after normalization, have the values $(1, 0, 0), (0, 1, 0), (0, 0, 1)$. From the three measured tristimulus values (K_k', L_k', M_k') the coefficients c_{ik}, i, $k = K, L, M$, of cross-talk matrix $\mathscr{C}$ can be calculated. Index k denotes the color of the pixel onto which the spot was projected and index i the color channel in which the signal was detected. For example, the first column of $\mathscr{C}$ follows from the measurement of a pixel of color K:

$$c_{KK} = 1 - c_{LK} - c_{MK}, \quad c_{LK} = \frac{L_K'}{K_K' + L_K' + M_K'},$$
$$c_{MK} = \frac{M_K'}{K_K' + L_K' + M_K'}. \tag{5}$$

Matrix $\mathscr{C}$ transforms the ideal tristimulus values (K, L, M) to real tristimulus values (K', L', M'), which are disturbed by color cross talk:

$$\begin{pmatrix} K' \\ L' \\ M' \end{pmatrix} = \begin{pmatrix} 1 - c_{LK} - c_{MK} & c_{KL} & c_{KM} \\ c_{LK} & 1 - c_{KL} - c_{ML} & c_{LM} \\ c_{MK} & c_{ML} & 1 - c_{KM} - c_{LM} \end{pmatrix} \times \begin{pmatrix} K \\ L \\ M \end{pmatrix}. \tag{6}$$

Because cross talk reduces contrast, all the coefficients of matrix $\mathscr{C}$ are positive. Color cross talk can be removed by the application of the inverse transform $\mathscr{C}^{-1}$ to the measured tristimulus vectors and the color transformation can be extended to include cross-talk compensation, $\mathscr{R}_{\text{PAL}}\mathscr{A}_{\text{opt}}\mathscr{C}^{-1}$. Thus color cross talk will not degrade colorimetric performance, but, because of the increased coefficients in the color transformation, a lower signal-to-noise ratio will result.

6. Influence of Quantization

Up to now all the estimations of colorimetric performance have been done under the assumption that matrixing is performed with floating point precision. But in the MASCOT CCD digital camera the signals are handled as integer values and quantization errors can introduce additional color errors. Therefore,

different combinations of digital dynamic range in the MASCOT camera are simulated.

The video signal from the CCD imager is digitized with a quantization of n_1 bits to obtain digital tristimulus values (K', L', M'). Intermediate sums and output values of the color transformation are limited to an n_2 bit and the final output values that appear at the output lookup table are rounded to n_3 bit. Table 1 summarizes the results of the simulation for different digital dynamic ranges n_1, n_2, n_3. The mean colorimetric errors ΔE hold for the transmission curves of Fig. 5(c) of the fabricated filters, illuminant D_{65}, and the optimized transformation $\mathscr{R}_{PAL}\mathscr{L}_{opt}$ for PAL RGB output data.

The camera was built with an input quantization n_1 of 10 bits, a quantization n_2 of matrixing of 16 bits, and an output quantization n_3 of 8 bits. As can be seen from Table 1 the limitation at the output introduces the main degradation in colorimetric performance, but the additional errors are so small that they can hardly be detected by human observers.

7. Experimental Results and Discussion

We tried to determine the color cross-talk compensation matrix $\mathscr{C}^{-1}$ after the procedure detailed in Section 5 in two different ways. First we measured the color cross talk on a masked black-and-white (b/w) CCD imager by the projection of small spots of light that were suitably prefiltered to exhibit the spectrum of light that entered a K, L, or M filter on the color imager. We obtained the following cross-talk matrix $\mathscr{C}_{b/w}$:

$$\mathscr{C}_{b/w} = \begin{bmatrix} 0.88 & 0.04 & 0.03 \\ 0.06 & 0.92 & 0.03 \\ 0.06 & 0.04 & 0.94 \end{bmatrix}. \tag{7a}$$

This measurement was repeated with a white-light spot on a color imager that, in addition, had the KLM colored stripe filter on top and obtained the following matrix $\mathscr{C}_{color}$:

$$\mathscr{C}_{color} = \begin{bmatrix} 0.94 & 0.06 & 0.24 \\ 0.04 & 0.90 & 0.16 \\ 0.02 & 0.04 & 0.60 \end{bmatrix}. \tag{7b}$$

The two matrices differ substantially and, while matrix $\mathscr{C}_{b/w}$ looks quite reasonable, matrix $\mathscr{C}_{color}$ shows a strong cross talk from the blue channel M into the green and red channels, which is not understood. We decided to measure the tristimulus vectors (K', L', M') of a large number of Colorcurve color samples with known spectra of reflectance and under a known spectrum of illuminance and to determine the cross-talk matrix by nonlinear optimization of matrixing. The color samples were measured under (45/0) illumination and viewing conditions[3] at a viewing angle of $\sim 1.5°$, which corresponds to a field of $\sim 3 \times 300$ detector pixels. We obtained the following cross-talk matrix $\mathscr{C}_{opt}$:

$$\mathscr{C}_{opt} = \begin{bmatrix} 1.21 & -0.01 & 0.14 \\ -0.09 & 0.91 & 0.30 \\ 0.08 & 0.03 & 0.43 \end{bmatrix}. \tag{7c}$$

Although $\mathscr{C}_{opt}$ differs largely from $\mathscr{C}_{b/w}$ and $\mathscr{C}_{color}$, it confirms the measurements we obtained from the color imager. In principle, the sums of the columns of cross-talk matrix $\mathscr{C}$ must be equal to one, and each coefficient must be positive. The nonlinear optimization of matrixing did not notice these restrictions but tried to minimize the resultant colorimetric errors as well as possible. In this way negative coefficients appeared, and the sum of each column was different from the valve one. Therefore, it was concluded that available data on the CCD response $s_{CCD}(\lambda)$, as provided by the CCD manufacturer at the beginning of this work, which was the only data we could not measure directly, were inaccurate, especially in the short-wavelength region. This suspicion was confirmed by a series of measurements of the relative sensitivity of the b/w imager at discrete wavelengths by using narrow-bandpass interference filters.

As a consequence the target filter curves no longer provide spectral responses of the color channels that are linear combinations of the color-matching functions $\bar{x}$, $\bar{y}$, $\bar{z}$. The mean colorimetric error of the MASCOT CCD digital camera prototype, which resulted after optimization of matrixing, was 2.65 jnd (CIELUV). This is slightly better than the performance of today's high-quality broadcast cameras. Visually the acquired images showed an exceptionally high colorimetric fidelity when they were displayed on a high-quality color monitor as well as a good uniformity over the whole field.

Table 1. Colorimetric Effect of Quantization in the MASCOT CCD Digital Camera

n_1	n_2	n_3	ΔE (jnd)	R_a
∞	∞	∞	1.0	97
12	16	10	1.0	96
10	16	10	1.1	96
12	16	8	1.2	96
10	16	8	1.3	96
10	14	8	1.3	96
8	16	8	2.0	92

8. Conclusion

A procedure for the development of color filters for precise color reproduction has been presented, which is based on colorimetric standards, computer simulation, and nonlinear optimization. Advanced design techniques for the dielectric filters allowed the use of filter transmission curves that ideally would not show systematic colorimetric errors and that were optimized to show no apparent color noise. The introduction of an additional global filter helped to reduce the requirements for the individual color filters and thus facilitated fabrication.

The transmission curves of the fabricated filters were in close agreement with the target curves and would cause a mean colorimetric error of only 1.3 jnd (CIELUV) if an optimized color transformation is applied that minimizes the color errors from the small deviations of the transmission curves and if quantization errors are taken into account.

The prototype camera showed a lower colorimetric performance than that predicted by simulation. Investigations showed that this was due to the filter design being based on available but slightly inaccurate input data of the imager's spectral response. Based on subsequent experimental data, the color transformation could be optimized to provide a mean colorimetric error of the actual camera system of ~2.7 jnd (CIELUV).

We gratefully acknowledge the help of many people at the Paul Scherrer Institute Zurich who contributed to the ESPRIT II MASCOT project and particularly to the present work. We express our appreciation to K. Knop for many stimulating discussions and for suggesting the global filter approach. We thank R. E. Kunz for providing the many computer designs that were required to determine the optimum dielectric filters and H. Brunner for actually fabricating them. We also thank J. M. Raynor for designing and building the hardware that was needed to take the measurements for characterizing and optimizing the MASCOT camera. In addition, we thank M. T. Gale for his continuing support and management of the MASCOT project, as well as for critically reading this manuscript. We also gratefully acknowledge the cross-talk measurements contributed by R. Zumbrunn and H. Gerber (Leica Heerbrugg). This work was supported in part by the Swiss Commission for the Advancement of Scientific Research, Project KWF-1804.2.

References

1. S. Suzuki, T. Kusunoki, and M. Mori, "Color characteristic design for color scanners," Appl. Opt. **29,** 5187–5192 (1990).
2. H. Brunner, K. Engelhardt, M. T. Gale, G. K. Lang, P. Metzler, J. M. Raynor, P. Seitz, L. Brissot, G. Cilia, C. Gadda, and V. Leone, "High fidelity, programmable CCD colour camera for desk-top publishing and the graphic arts," in *Proceedings of the Annual ESPRIT Conference 1991* (Commission of the European Communities, Luxembourg, 1991), pp. 439–454.
3. G. Wyszecki and W. S. Stiles, *Color Science: Concepts and Methods, Quantitative Data and Formulae,* 2nd ed. (Wiley, New York, 1982), Chap. 3.
4. K. Knop and R. Morf, "A new class of mosaic color encoding patterns for single-chip cameras," IEEE Trans. Electron Devices **ED-32,** 1390–1395 (1985).
5. R. Morf and R. E. Kunz, "Dielectric filter optimization by simulated thermal annealing," in *Surface Measurement and Characterization,* J. M. Bennett, ed., Proc. Soc. Photo-Opt. Instrum. Eng. **1019,** 211–217 (1988).
6. R. Morf and R. E. Kunz, "Dielectric filter optimization by simulated thermal annealing: a simulated zone-melting approach," in *Optical Thin Films and Applications,* R. Herrmann, ed., Proc. Soc. Photo-Opt. Instrum. Eng. **1270,** 11–17 (1990).
7. J. M. Raynor and P. Seitz, "The technology and practical problems of pixel-synchronous CCD data acquisition for optical metrology applications," in *Close-Range Photogrammetry Meets Machine Vision,* E. Baltsavias and A. Gruen, eds., Proc. Soc. Photo-Opt. Instrum. Eng. **1395,** 96–103 (1990).
8. A. H. Jones, "Optimum color analysis characteristics and matrices for color television cameras with three receptors," J. SMPTE **77,** 108–115 (1968).
9. *Colorcurve Master Atlas* (Colorcurve Systems, Inc., Minneapolis, Minn., 1988).
10. D. L. MacAdam, *Color Measurement,* Vol. 27 of Optical Sciences (Springer-Verlag, Berlin, 1981), pp. 64–65.
11. M. T. Gale, H. W. Lehmann, H. Brunner, and K. Frick, "*In-situ* optical monitoring of thin films during evaporation," in *Surface Measurement and Characterization,* J. M. Bennett, ed., Proc. Soc. Photo-Opt. Instrum. Eng. **1019,** 90–95 (1988).